Research Article

Open Access

Jaroslav Hofierka* and Monika Knutová

Simulating spatial aspects of a flash flood using the Monte Carlo method and GRASS GIS: a case study of the Malá Svinka Basin (Slovakia)

Abstract: This paper focuses on the flash flood assessment using a spatially-distributed hydrological model based on the Monte Carlo simulation method. The model is implemented as r.sim.water module in GRASS GIS and was applied to the Malá Svinka Basin in Eastern Slovakia where a heavy rainfall (100 mm/hr.) caused a flash flood event with deadly consequences in July 1998. The event was simulated using standard datasets representing elevation, soils and land cover. The results were captured in time series of water depth maps showing gradual changes in water depths across the basin. The hydrological effects of roads in the study area were simulated using the preferential flow feature of the model. This simulation helped to identify source areas contributing to flooding in built-up areas. The implementation in a GIS environment simplifies the data preparation and eventual modification for various scenarios and flood protection measures. The simulation confirmed excellent robustness and flexibility of the method.

Keywords: flash flood; overland flow; Monte Carlo; GRASS GIS; SIMWE

1 Introduction

Flash floods are among the most dangerous natural hazards with possible significant damages and human casualties. They are usually generated by extreme rainfall events with high intensities shortly followed by a strong and fast flow. Flash floods usually affect smaller basins (tens to hundreds km^2) with shorter hydrologic response times. The local character of flash floods and the typical lack of meteorological and hydrological measurements in the affected area pose several problems when analyzing such events. Besides the heavy rainfall, there are also other factors influencing occurrence of the local floods such as topography, land cover, and soil [1–4]. Moreover, the state of land cover and soil varies substantially throughout the year with quite a strong impact on the runoff [5].

Various factors affect the phenomenon, therefore a complex geographical database representing all components of the landscape is needed to account for the factors. Over the last decades, a geographic information system (GIS) technology has been widely used to represent landscapes. GIS also provides basic tools for data transformation to prepare input data for further geospatial analysis or modeling. The hydrologic modeling can be performed using models which are implemented in a separate software, for example, the models developed by the Hydrologic Engineering Center (HEC) in Davis, California or MIKE developed by the Danish Hydrologic Institute (DHI)[1]. In this case, the spatial data prepared in GIS are imported into the specialized software. Alternatively, these models can be integrated into a GIS environment in the form of a GIS command, for example, r.hydro.CASC2D in GRASS GIS [6]. Full integration with GIS provides more flexibility in terms of data preparation and availability of geospatial methods and procedures. On the other hand, the independent hydrological software is under full control of the developer. The recently very popular open-source concept in software development has also had an influence on the development of hydrological components of GIS software such as GRASS GIS or SAGA[2] [3].

GRASS GIS is an open-source geospatial software consisting of modules dedicated to support solving various geospatial issues. It is quite commonly used in environmental modeling including hydrological applications. It includes several hydrological modules, such as

***Corresponding Author: Jaroslav Hofierka:** Institute of Geography, Faculty of Science, Pavol Jozef Šafárik University in Košice, Jesenná 5, 04001 Košice, Slovak Republic, E-mail: jaroslav.hofierka@upjs.sk
Monika Knutová: Družstevná 37, 08006 Prešov, Slovak Republic

r.topmodel, r.water.fea, r.hydro.CASC2d, r.sim.water². The open-source concept makes GRASS GIS especially attractive for researchers who can freely modify the source code and develop new modules in interaction with other software developers and users [7]. The r.sim.water and r.sim.sediment modules [8, 9] are excellent examples of the interaction and coordinated development of highly sophisticated modeling tools. The modules represent a direct implementation of the SIMulated Water Erosion (SIMWE) model that was developed for spatially-distributed soil erosion modeling based on the Water Erosion Prediction Project (WEPP) and Unit Stream Power-based Erosion Deposition (USPED) soil erosion models [10]. The SIMWE model uses the Monte Carlo simulation approach based on approximation of the underlying physical principles and equations representing the phenomenon (the Saint-Venant equations). While the SIMWE model is not directly a flood model, it simulates the overland flow phenomenon that directly contributes to the flooding especially in small basins. The approach can better explain the spatial processes contributing to the water flow in river channels. Recently, the kinematic wave models are often used in flood runoff estimations on drainage basins [5].

The aim of the paper is to demonstrate the applicability of the Monte Carlo approach and r.sim.water module in GRASS GIS in the simulation of flash flood events using the example of the Malá Svinka Basin in Slovakia. We also demonstrate the capability of the model for simulating the hydrological effects of roads affecting the flood event using the preferential flow feature.

2 Methods

2.1 The hydrological component of the SIMWE model

The SIMWE model is a process-based and spatially-distributed model that has two main components: (i) a hydrological and (ii) erosion component, both implemented in GRASS GIS as r.sim.water and r.sim.sediment, respectively [8, 10]. In this paper, we are focusing on the hydrological component of the SIMWE model and its applicability to flash flood modeling in small basins.

In this model, the hydrological component simulates the overland flow described by the bivariate form of the Saint Venant continuity equation [10, 11]:

$$\frac{\partial h(\boldsymbol{r}, t)}{\partial t} = i_e(\boldsymbol{r}, t) - \nabla . \boldsymbol{q}(\boldsymbol{r}, t), \qquad (1)$$

where $\boldsymbol{r} = (x, y)$ [m] is the position, t [s] is the time, $h(\boldsymbol{r}, t)$ [m] is the depth of overland flow, $i_e(\boldsymbol{r}, t)$ [m/s] is the rainfall excess = (rainfall − infiltration − vegetation intercept) [m/s], $\boldsymbol{q}(\boldsymbol{r}, t)$ [m²/s] is the water flow per unit width. The momentum conservation in the diffusion wave approximation has the following form [9, 10]:

$$\boldsymbol{s}_f(\boldsymbol{r}, t) = \boldsymbol{s}(\boldsymbol{r}) - \nabla h(\boldsymbol{r}, t), \qquad (2)$$

where $\boldsymbol{s}(\boldsymbol{r}) = -\nabla z(\boldsymbol{r})$ is the negative elevation gradient, $z(\boldsymbol{r})$ [m] is the elevation, and $\boldsymbol{s}_f(\boldsymbol{r}, t)$ is the negative gradient of overland flow surface (friction slope). If the hydraulic radius is approximated by the normal flow depth $h(\boldsymbol{r}, t)$, then the unit discharge is given by [5]:

$$\boldsymbol{q}(\boldsymbol{r}, t) = \boldsymbol{v}(\boldsymbol{r}, t) h(\boldsymbol{r}, t), \qquad (3)$$

where $\boldsymbol{v}(\boldsymbol{r}, t)$ [m/s] is the flow velocity. The system of equations (1) − (3) is closed using the Manning's relation between $h(\boldsymbol{r}, t)$ and $\boldsymbol{v}(\boldsymbol{r}, t)$ [9, 10]:

$$\boldsymbol{v}(\boldsymbol{r}, t) = \frac{C}{n(\boldsymbol{r})} h(\boldsymbol{r}, t)^{2/3} \left| \boldsymbol{s}_f(\boldsymbol{r}, t)^{1/2} \right| \boldsymbol{s}_{f0}(\boldsymbol{r}, t), \qquad (4)$$

where $n(\boldsymbol{r})$ is the dimensionless Manning's coefficient, $C = 1$ [m$^{1/3}$/s] is the corresponding dimension constant and $\boldsymbol{s}_{f0}(\boldsymbol{r}) = \boldsymbol{s}_f(\boldsymbol{r})/\left| \boldsymbol{s}_f(\boldsymbol{r}) \right|$ is the unit vector in the friction slope direction. The kinematic wave approximation of continuity and momentum equations for a steady water flow assumes that

$$\frac{\partial h(\boldsymbol{r}, t)}{\partial t} = 0.$$

In that case

$$\nabla \left[h(\boldsymbol{r}, t) \boldsymbol{v}(\boldsymbol{r}), \right] = i_e(\boldsymbol{r}). \qquad (5)$$

In order to incorporate the diffusive wave effects at least in an approximate way, Mitas and Mitasova [10] proposed to introduce a diffusion-like term $\propto \nabla^2 \left[h^{5/3}(\boldsymbol{r}) \right]$ into equation (5):

$$-\frac{\varepsilon(\boldsymbol{r})}{2} \nabla^2 \left[h^{5/3}(\boldsymbol{r}) \right] + \nabla \left[h(\boldsymbol{r}, t) \boldsymbol{v}(\boldsymbol{r}, t) \right] = i_e(\boldsymbol{r}), \qquad (6)$$

where $\varepsilon(\boldsymbol{r})$ is a spatially variable diffusion coefficient. This diffusion term improves the kinematic solution by overcoming small shallow pits common in digital elevation models (DEM) and by smoothing out the flow over abrupt changes in terrain or Manning's roughness coefficient. Such abrupt changes (e.g., roads, land cover) are quite common in real landscape and should be captured by the simulation. However, they often negatively affect the numeric stability of traditional approximation methods, such as finite difference methods [6].

2.2 The Monte Carlo numerical solution

The Saint Venant equations are solved by a stochastic method called Monte Carlo (very similar to Monte Carlo methods in computational fluid dynamics). It is assumed that these equations are a representation of stochastic processes with diffusion and drift components (Fokker-Planck equations). The Monte Carlo technique has several unique advantages. The first is the robustness which enables us to solve the equations for complex cases, such as discontinuities in the coefficients of differential operators (in our case abrupt slope or cover changes). The second benefit is in the speed of calculation as any rough solutions can be estimated quite quickly. Thirdly, one can take the advantage of scalability from a single workstation to large parallel machines due to the independence of sampling points[2] [9]. The concept of sampling points and related concept of duality between the field and particle representation of the modelled phenomenon brings a whole range of new simulation methods to landscape modeling using GIS. In this concept, the quantity is computed (sampled) with high density in every cell of the grid representing the phenomenon. Then the particle representation can be replaced by a continuous approximation of the phenomenon using a physical field. The initial particle density should be at least 2 particles per a grid cell to ensure a smooth representation of the water flow simulated by r.sim.water, [9].

2.3 Implementation in GRASS GIS

The SIMWE model has been implemented in GRASS GIS in two software modules linked together via the SIM library. The r.sim.water module simulates the overland flow and the r.sim.sediment module estimates the sediment flow and net erosion-deposition rates using the output from the r.sim.water module [8]. The key inputs for the r.sim.water module include the following grid maps: elevation, water flow gradient (defined by the first-order partial derivatives of the elevation map), rainfall excess rate and a surface roughness coefficient given by Manning's n. The partial derivatives of the elevation field can be computed during the interpolation by the v.surf.rst module or, if the elevation grid is already provided, using the r.slope.aspect module. Partial derivatives are used to determine the direction and magnitude of water flow velocity. This can be effectively used to define the direction of the water flow in certain locations such as man-made landscape features that act like a drainage network (e.g., channels, ditches or culverts) even if they do not follow the elevation gradient. The

resulting vector field $w(r)$ representing the flow direction in the entire area of interest is then defined as [8]:

$$w(r) = (1 - \delta_{ij})w_e(r) + \delta_{ij}w_d(r), \qquad (7)$$

where $w_e(r)$ is the vector in the steepest slope direction derived from a DEM, $w_d(r)$ is the vector representing the flow in the drained landscape features and δ_{ij} is the Kronecker delta. Partial derivatives needed to define the $w_d(r)$ vector can be derived as follows:

$$
\begin{aligned}
w_x &= \tan(\gamma)\cos(\alpha), \\
w_y &= \tan(\gamma)\sin(\alpha), \qquad (8)
\end{aligned}
$$

where γ and α are the feature slope and flow direction, respectively. The resulting vector field $w(r)$ can be easily derived using standard GIS map algebra operations as a combination of two maps.

The simulation includes a diffusion term parameter (Equation (6)) which enables water flow to overcome elevation depressions or obstacles when water depth exceeds a threshold water depth value. When this threshold value is reached, the diffusion term increases by a chosen value and water flow continues in a more diffusion-like movement. The effects of flood protection and mitigation measures such as check dams or similar type of structures can be simulated using a raster map with values representing the permeability of the measures. The permeability values (0-1) express the probability of particles to pass through the structure.

Rainfall excess is defined as the difference between rainfall intensity and infiltration rate [mm/hr] and therefore it is highly spatially and temporally variable. Rainfall intensities are usually available from meteorological stations or estimated using radar measurements. Infiltration rate depends on soil properties and land cover. For saturated soil and steady-state water flow it can be estimated using saturated hydraulic conductivity rates based on field measurements or using reference values which can be found in literature. In the r.sim.water module, the rainfall excess can be defined using a raster-based map with spatially distributed values. The module simulates the overland flow even if the rainfall excess affects only a part of the studied area. This is useful for smaller rainfall events or in areas with strongly varying soil and land cover properties. The current implementation of the model (GRASS version 7.0) still lacks a temporally variable definition of rainfall excess. Although its implementation is possible the input of temporally variable rainfall excess would require a time-series of raster maps increasing the complexity of data preparation.
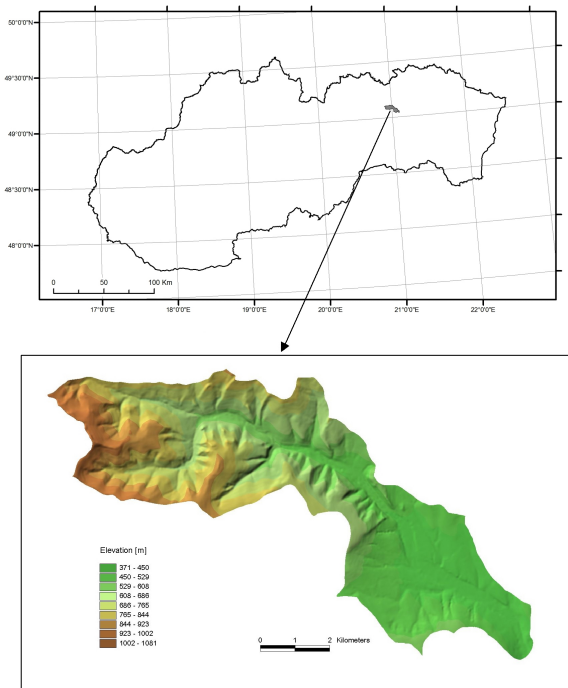
Figure 1: Position and elevation map of the study area.

The Manning's roughness coefficient controls the velocity of overland flow (Equation (4)). The estimation of this parameter for natural surfaces is often a source of uncertainty. Natural surfaces usually consist of various elements such as soil surface, rocks, standing vegetative material, that contribute to the total hydraulic resistance of the particular land cover class. It is nearly impossible to measure the value over large and complex landscape areas, therefore the estimation of the parameter is based on approximate values and calibration using the hydrological response of the basin [12].

The r.sim.water output includes a water depth grid map [m], and a water discharge grid map [m^3/s]. The error of the numerical solution can be analyzed using the simulation error grid map which is defined as the root mean square error of the resulting average water depth. The output water depth and discharge maps can be saved during the simulation using a time series parameter defining the time step in minutes for writing output files.

3 Study area and dataset

The study area is located in Eastern Slovakia (49°05′N, 21°00′E), about 20 km to the north-west of the city of Prešov. The study area comprises the upper part of the Malá Svinka Basin (44.5 km^2) from the spring of
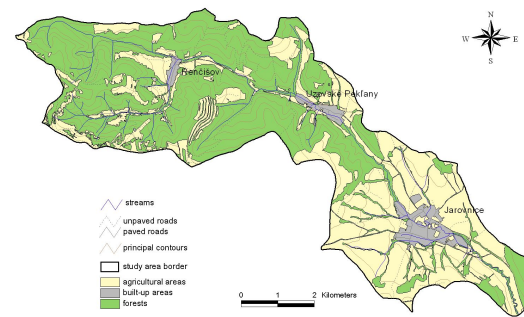
**Figure 2:** Topographic map of the study area.

the river to its outlet at the Lažany village. The elevations are in the interval of 371 - 1081 m a.s.l. (Figure 1). The bedrock comprises the Central Carpathian Paleogen unit with sandstones and clay flysch formations. The cambisol soil class with loam and sandy-loam soil textures dominates in the agricultural areas. More than 50% of the area is covered by forests dominated by broad-leaf deciduous forests, only areas with higher elevations are occupied by a coniferous forests. The built-up areas represent villages with complex patterns of residential houses, gardens and roads (Figure 2).

3.1 Input data

The input data for the r.sim.water module were derived from publicly available datasets, such as topographic maps, soil maps and orthophotomaps. Digital elevation model (DEM) was derived from the vectorized contours of the topographic map of the 1:10 000 scale using the v.surf.rst spatial interpolation module in GRASS GIS. The spatial resolution of the grid-based DEM was set to 10 m which reflects the scale of the source topographic map. The soil maps in the ESRI shapefile vector format were provided by the Slovak Soil Conservation Service VÚPOP Bratislava. The land cover map and the road network was derived from the orthophotomap at 1-m spatial resolution from the years 2002 and 2003 provided by VÚPOP Bratislava.

These primary data sets were reclassified into input grids for the r.sim.water module using standard GIS operations in GRASS GIS, such as r.reclass, r.recode or r.mapcalc [7]. The reclassification rules were taken from previous studies and recommended values published in [8, 13, 14]. The roughness effect of land cover classes was expressed via Manning's n based on the recommended values by En-
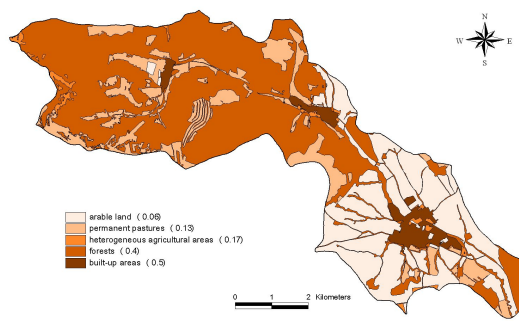
Figure 3: Manning's roughness coefficient based on land cover.

gman [13]. The Manning's n value for a built-up area (a complex mixture of buildings, gardens, fences, etc.) was estimated based on the study by Syme [14] (Table 1, Figure 3). Infiltration rates are the most difficult to estimate. They vary greatly depending on the initial soil condition, soil pore structure and land cover. In our study area, the land cover is the most important factor affecting the spatial variation of infiltration rate. Kidwell et al. [15] documented that vegetal cover on rangelands is positively correlated with infiltration. Using this assumption, the infiltration rate values were roughly estimated using soil and land cover data (Table 1). Vegetation intercept was not explicitly considered in this study.

The flood was simulated using a uniform rainfall intensity of 100 mm/hr replicating the heavy rainfall event with a cumulated rainfall depth of 100 mm in 1 hour that occurred on July 20, 1998 as estimated by the Slovak Hydrometeorological Institute, Bratislava, using the data from a Doppler radar (Table 1). As reported by the Slovak Water Management Company SVP, Košice, a 4-m flood wave hit several villages in the area with very tragic consequences in the Jarovnice village (around 50 human casualties). According to Svoboda and Pekárová [16], there is no rain-gauge or hydrometric stations the study area therefore hydrologic estimations were made using post-flood surveys and simulations.

4 Results and discussion

The r.sim.water module with the input data presented above was applied in order to analyze spatial aspects of the simulated flash flood event in the study area. The speed of simulation was about 3 minutes on a standard PC depending on the number of time-series output data files
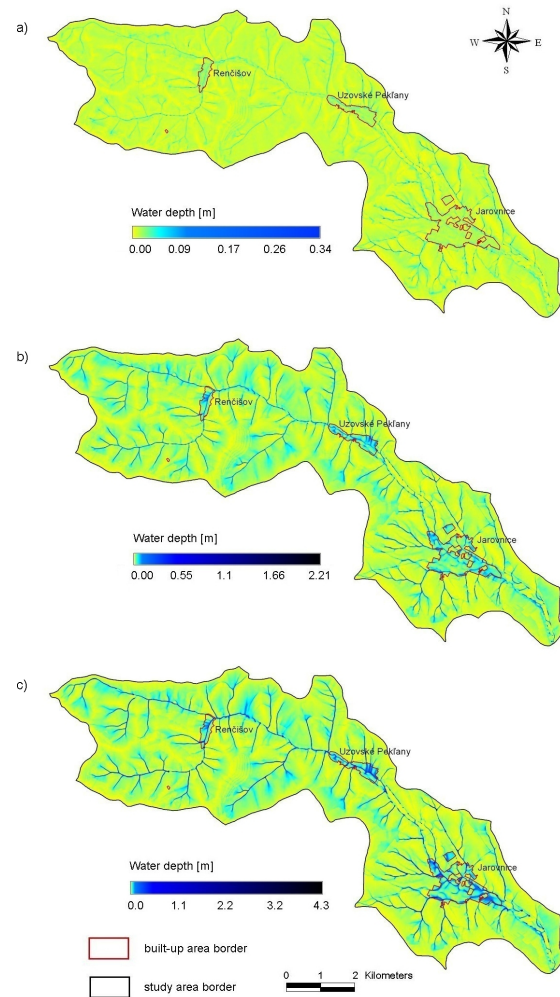
Figure 4: Simulated water depth after a) 5 min., b) 20 min., c) 60 min.

saved in the database. The internally calculated time step used in the simulation was 2.68 seconds. The robustness of the Monte Carlo method provided an excellent numerical stability of the calculation. No further modification of the data was necessary even though various imperfections were present in the data (e.g., pits in DEM) that can cause instability issues in traditional numerical methods.

The r.sim.water module simulates the overland flow based on rainfall excess. In our case the intensity of the rainfall event was very high (100 mm/hr.), therefore overland flow was generated in all parts of the area with varying intensity (Table 1). The spatial distribution of water depth over time depends on factors affecting the flow routing. We selected 3 time horizons: 5th, 20th and 60th minute from the start of the simulation to document the simulated dynamics of the event. Figure 4 shows the simulated changes in water depth in these 3 time horizons. Fig-

Table 1: Input parameters for the simulated flash flood event.

Land cover	Manning's roughness coefficient	Rainfall intensity [mm/hr]	Infiltration rate [mm/hr]	Rainfall excess [mm/hr]
forest	0.4	100	50	50
permanent pastures	0.13	100	35	65
arable land	0.06	100	20	80
heterogeneous agricultural areas	0.17	100	35	65
built-up areas	0.5	100	20	80

ure 4a shows a water depth map in the 5th minute. Comparison with Figure 3 reveals that the areas with a lower infiltration and retention capacity (agricultural areas) are quickly increasing the amount of water and gradually concentrating water in valleys. The next time horizons (Figure 4b-c) show that overland flow reaches a steady-state in various times in different parts of the basin. The steady-state is quickly reached in upper parts of the basin in agricultural areas, whereas the process is slower in forests and lower parts of the basin (valleys). Comparison of Figure 4b and 4c shows that the upper parts of the basin quickly reach a steady-state condition; only the lower parts of the basin close to the Jarovnice village still exhibits an increase in water depth. The highest water depth levels reaching 4.3 m were simulated in the main valley in the 60th minute. Similar value (4 m) was reported by the Slovak Water Management Company SVP, Košice, for the real event on July 20, 1998.

In order to exploit the unconventional functionality of the r.sim.water module using a preferential flow, we also simulated possible drainage effects of unpaved and paved roads in the selected area near Jarovnice village (Figure 5). Each road was inspected in terms of possible drainage effects and, if selected, the values of water flow gradient in the cells representing the road were changed according to the expected direction of flow along these roads. Figure 5 a) represents the simulation for the 60th minute without the preferential flow and effects of roads, Figure 5b) represents the same time horizon with the preferential flow on roads.

Figure 5 shows the effects of roads on overland flow in the selected area. The roads act as barriers and drainage lines depending on the morphology and spatial resolution of the elevation data. They change the direction of the overland flow originally defined by the elevation gradient. In several cases, the road concentrates the flow and increases the amount of water flowing to the built-up area. For example, in Jarovnice, several roads concentrate the water flow coming to the built-up area leading to increased water depths in the built-up area (locations A and B). In comparison, the location C is not substantially influenced by roads and the water depths predicted by the simulation with and without preferential flow are almost the same. Figure 5b) also shows the effects of a raster data model causing concentrated overflow when some particles reach the cell of the raster off the road. Depending on the actual draining effect of the road, this can be controlled by modifying the direction of flow according to the regular structure of raster and the diffusion parameter in Equation eqrefe:6. This example also demonstrates that the simulation can be very detailed depending on the resolution and accuracy of input data.

The simulation does not contain a channel network representing streams in the area. However, the application of this spatially distributed rainfall-runoff model helps to better understand the sources of flooding in the channels. High-resolution data coupled with flexibility and robustness of the model enable assessment of risks and provide means for effective planning of flood protection and mitigation measures such as ditches or check dams. Such tasks, however, will require a higher spatial resolution of input data capturing variations in elevation and size of the protection measures (1-2 meters). Gallay et al. [17] discuss various modern methods for creating high-accuracy DEMs including laser scanning that might be necessary in such detailed simulations.

5 Conclusions

Detailed spatial analysis of water flow in a basin can be effectively used in planning flood protection measures. The measures should be organized in such a manner that would help to minimize the peak of the flood wave. This can be achieved by areal land cover changes improving the infiltration and retention of water in the upper parts of the basin or other flood protection measures to slow down the
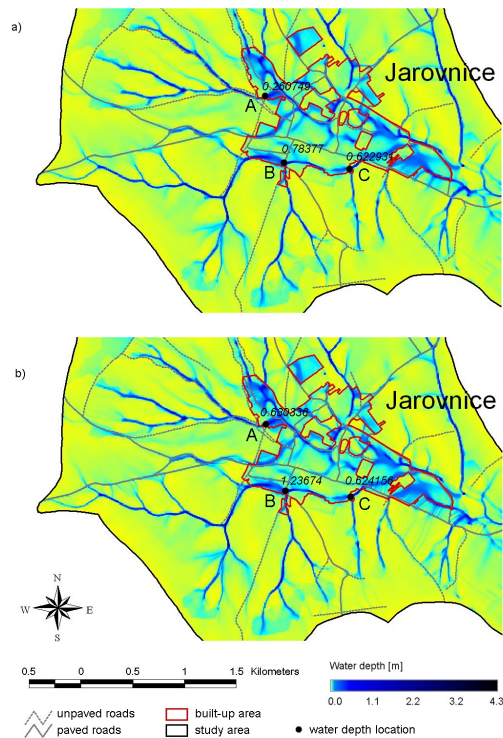
Figure 5: The effects of roads on simulated water depths a) without preferential flow, b) with preferential flow.

water flow. The GIS environment with all necessary tools to modify input data greatly helps to prepare such scenarios and to analyze the effects in certain areas within the basin.

The presented model shows that the Monte Carlo methodology is very flexible and robust for various landscape configurations. Such models can be very effectively used to assess the effect of flood protection measures such as dams, ditches or culverts. The effect of such prevention measures is often very difficult to simulate using traditional modeling techniques.

The presented simulation model implemented as r.sim.water in GRASS GIS was successfully applied in the study area of the Malá Svinka Basin with the following results and conclusions:

a) The model is spatially-distributed enabling identification of areas contributing to the flood event in specific places.

b) The implementation in GRASS GIS environment provides the necessary tools and simplifies data preparation and eventual modification for various scenarios and flood protection measures.

c) The preferential flow feature extends the common functionality of similar models toward a more detailed analysis of water flow effects of various landscape features or flood prevention measures. However, this requires high-

resolution input data and computational techniques such as laser scanning and high-performance parallel processing.

References

[1] Marchi, L., Borga, M., Preciso, E., Gaume, E., Characterisation of selected flash floods in Europe and implications for flood risk management, J. Hydrol., 2010, 394, 118–133.
[2] Loóczy, D., Czigány, S., Pirkhoffer, E., Flash Flood Hazards, In: Kumarasamy, M. (Ed.) Studies on Water Management Issues, In-Tech, 2012.
[3] Solín, L., Feranec, J., Nováček, J., Land cover changes in small catchments in Slovakia during 1990-2006 and their effects on frequency of flood events, Nat. Hazards, 2010, 56, 195–214.
[4] Minea, G., Assessment of the Flash Flood Potential of Basca River Catchment (Romania) Based on Physiographic Factors. Cent. Eur. J. Geosci., 2013, 5, 344–353.
[5] Maidment, D.R., Handbook of Hydrology, McGraw-Hill, New York, 1993.
[6] Saghafian, B., Implementation of a distributed hydrologic model within Geographic Resources Analysis Support System (GRASS), Proceedings of the Second International Conference on Integrating Environmental Models and GIS, Breckenridge, CO, USA, 1993.
[7] Neteler, M., Mitasova, H., Open Source GIS: A GRASS GIS Approach, Third Edition, The International Series in Engineering and Computer Science: Vol. 773, Springer New York Inc., 2008.
[8] Hofierka, J., Mitasova, H., Mitas, L., GRASS and modeling landscape processes using duality between particles and fields. In: Ciolli M., Zatelli P. (Eds.): Proceedings of the Open Source Free Software GIS - GRASS users conference 2002, Trento, Italy 11-13 September, 2002.
[9] Mitasova, H., Thaxton, C., Hofierka, J., McLaughlin, R., Moore, A., Mitas L., Path sampling method for modeling overland water flow, sediment transport and short term terrain evolution in Open Source GIS. In: C.T. Miller, M.W. Farthing, V.G. Gray, G.F. Pinder (Eds.): Proceedings of the XVth International Conference on Computational Methods in Water Resources (CMWR XV), June 13-17 2004, Chapel Hill, NC, USA, Elsevier, 2004, 1479–1490.
[10] Mitas, L., Mitasova, H., Distributed soil erosion simulation for effective erosion prevention, Water Resour. Res. 1998, 34, 505–516.
[11] Julien, P. Y., Saghafian, B., Ogden, F. L., Raster-based hydrologic modeling of spatially-varied surface runoff. Water Resour. Bull., AWRA, 31, 1995, 523–536.
[12] Vieux, B.E., Distributed Hydrologic Modeling Using GIS, Kluwer Academic Publishers, Dordrecht, Water Trans. 48, 2004.
[13] Engman, E.T., Roughness coefficient for routing surface runoff. J. Irrig. Drain. Eng., 1986, 112, 39–53.
[14] Syme, W.J., Flooding in urban areas - 2D modelling approaches for buildings and fences. In: Engineers Australia, 9th National Conference on Hydraulics in Water Engineering, Darwin Conven-

tion Centre, Australia, 2008.

[15] Kidwell, M.R., Weltz, M.A., Guertin, D.P., Estimation of Green-Ampt effective hydraulic conductivity for rangelands, J. Range Manage., 1997, 50, 290–299.

[16] Svoboda A., Pekárová P., Katastrofálna povodeň z júla 1998 v povodí Malej Svinky - simulácia jej priebehu, Catastrophic flood of July 1998 in the Malá Svinka catchment - its simulation.

J. Hydrol. Hydromech., 1998, 46, 356–365 (in Slovak with English summary).

[17] Gallay, M., Lloyd, C. McKinley, J., Barry, L., Assessing modern ground survey methods and airborne laser scanning for digital terrain modelling: A case study from the Lake District, England. Comput. Geosci., 2013, 51, 216–227.